PERGAMON

Available online at www.sciencedirect.com

SCIENCE DIRECT®

International Journal of Impact Engineering 30 (2004) 639–663

INTERNATIONAL JOURNAL OF IMPACT ENGINEERING

www.elsevier.com/locate/ijimpeng

Adaptive crashworthiness concept

Jan Holnicki-Szulc[a,]*, Lech Knap[b]

[a] Institute of Fundamental Technological Research, Warsaw, Poland

[b] Warsaw University of Technology, Warsaw, Poland

Received 5 September 2002; received in revised form 13 August 2003

Abstract

A design methodology for adaptive structures (structures equipped with controllable dissipaters) with high crashworthiness performance is proposed. A numerical package capable of solving particular problems, i.e. (i) crashworthiness analysis of structure with fixed properties of dissipaters, (ii) optimal remodelling of adaptive structure and (iii) optimal design of yield stress levels triggering plastic-like distortions in dissipaters, is presented and verified using test examples.

Some general, quantitative conclusions and suggestions for further applications of the adaptive crashworthiness concept are formulated.

Keywords: Adaptive structures; Crashworthiness; Structural control; Optimal design

1. Introduction

The important problem of safe vehicle design with an maximum impact energy dissipation is an intensive research subject (cf. the problem of crashworthiness analysis of rail vehicles [1–5]). Typically, the suggested solutions focus on the design of passive energy absorbing systems. These systems are frequently based on aluminium and/or steel honeycomb packages characterised by a high-specific energy absorption ratio. However high the energy absorption capacity of such elements are, they still remain highly redundant structural members which do not carry any load in an actual operation of a given vehicle. In addition, passive energy absorbers are designed to work effectively in pre-defined collision scenarios. For example, the frontal honeycomb cushions are very effective during a symmetric axial crash (or telescoping) of colliding coaches when the train remains on the rails, but are completely useless in other types of crash loading such as, e.g.,

*Corresponding author.

E-mail address: holnicki@ippt.gov.pl (J. Holnicki-Szulc).

0734-743X/$ - see front matter
doi:10.1016/j.ijimpeng.2003.08.004

'jack-knifing' after the train has left the rails. Consequently, distinct and sometimes completely independent systems must be developed for specific collision scenarios.

In contrast to the standard passive systems, the proposed research focuses on *active adaptation* of energy absorbing structures where the system of sensors recognises the type of crash loading and activates energy absorbing components in the sequence that guarantees optimal dissipation of impact energy.

Nowadays the numerical simulation tools used in routine engineering practice focus on the *precise calculation* of the crashing response of pre-defined structures, but offer little guidance in the *design process* of an optimal, complex energy absorbing system [6–10]. The corresponding methodology (and the software package) will be described in the present paper. As a result, the optimal material distribution as well as non-linear material characteristics can be designed (with help of the postulated methodology) for a predicted set of crash scenarios, including side impacts. These ideal, non-linear material characteristics can be approximated with use of passive techniques or more efficiently (however costly) in a semi-active way.

A two-level design concept for dynamically adaptive support structure of a railway car is proposed (Fig. 1a) as a testing model for verification of the dynamic adaptation concept. The bottom supporting structure (1 in Fig. 1a) is destined to sustain a crash impact (in a controlled way) without constraints imposed on accelerations, while the task for the secondary suspension system (2 in Fig. 1a) is to slow down accelerations in the car body for protection of passengers and carried goods. The subject of this paper concerns design of this bottom, skeletal, dynamically adaptive supporting structure equipped with special devices (the so-called *dissipaters* or *dynamic structural fuses*) in all members. We assume that these structural fuses can be activated when an arbitrarily chosen local stress level σ^* is reached and then an ideal plastic-like behaviour of the structural member can be performed (Fig. 1c). Concerning our considerations to truss structures

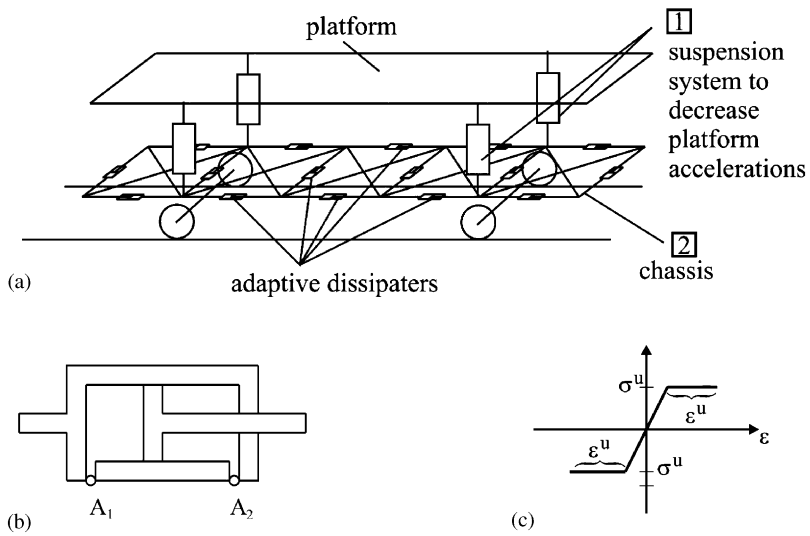

Fig. 1. (a) Two-level design concept for dynamically adaptive structure; (b) model of hydraulic adaptive dissipater and (c) characteristics of adaptive member.

(however, the concept can be generalised for frame type of structures as well) we will discuss dynamic behaviour of ideal elasto-plastic trusses with the yield stress levels σ^* chosen below the stresses σ^U causing failures in the structural elements.

In truss structures the model of an energy-dissipating device can be described as a piston with controlled valves opening the fluid flow (Fig. 1b). Assume that characteristic of an element (Fig. 1c) defines desired maximum upper and lower limit values $\sigma^U, \sigma^L = -\sigma^U$ beyond which a plastic behaviour occurs. The dissipater device, controlled (by opening if it is necessary valve A_1 or A_2) to keep pressures in the cylinder (Fig. 1a) $p_1 \leqslant \sigma^L$ and $p_2 \leqslant \sigma^U$, provokes plastic-like overall behaviour (simulated by *plastic distortions* ε^0) of the member. In this way, the original structure equipped with dissipaters can behave like an ideal elasto-plastic structure with a controllable limit stress level. In real applications, however, it is more likely that devices with an easy controllable MRF (magneto rheological fluid, [17]) will be used as adaptive energy absorber.

No restrictions on velocity of plastic-like flow in dissipaters are taken into account in the current stage of consideration. However, note that fully passive (with no time delay control problems) realisation of the dynamically adaptive design concept is also possible. In this case, structural elements should be equipped with specially designed inclusions (e.g., honeycomb-like parts built into structural members) causing overall characteristic of members as in Fig. 1c.

An important feature of the proposed concept is dissipative character of actuation. It means that always $\sigma_i \Delta\varepsilon_i^0 \geqslant 0$, and therefore, no external energy sources are required to "move" actuators.

The main point in the design of dynamically adaptive structure is incorporation of the largest portion of the structure to the controlled flow process in order to protect the structure against failure.The aims of this paper are:

- to determine crash-worthiness limits for an ideal adaptive structure with constant, elasto-plastic properties and local plastic flow value limited
- to propose a methodology for the determination of crash-worthiness limits for adaptive structure with actively controlled properties of dissipaters.

The applied approach (based on the so-called *Virtual Distortion Method*, VDM, [11,12] allows development of an efficient computational method for numerical dynamic analysis of elasto-plastic structures modelling behaviour of adaptive structures equipped with controlled (due to characteristics from Fig. 1c) dissipaters. In each time step of analysis (the transient problem) the stress redistribution due to plastic zone's development can be done through a sequence of corrections to the deformation field. These corrections are realised through *virtual distortions* (free of any geometrical and statistical constraints) and corresponding states of compatible deformations and self-equilibrated forces. Constraining our considerations to small deformations (on this stage of presentation), the global non-linear behaviour of the structure is obtained from superposition of linear elastic and residual states and thus reformation of the global stiffness matrix is not required. These residual states can be efficiently determined with help of pre-computed, so-called *influence matrix* ***D***, denoting structural response for locally generated unit virtual distortions. The proposed VDM technique can be generalised for the case of large deformations. On the other hand, it can be applied also to simulation of material redistribution [11] and to the complex smart structure design (remodelling and stress limits adaptation) problem.

Finally, note the following comments:

Adaptive members can be realised as ordinary load-bearing members, but equipped with special joints allowing overall performance described by characteristics shown in Fig. 1c. It is assumed that all structural members can be adaptive. Nevertheless, an alternative problem formulation can be proposed with reduced number of optimally located adaptive members, in order to find more economical (but still effective) solution.

In the considered example of two-level design concept for dynamically adaptive structure (Fig. 1a and the numerically simulated model, Fig. 8) we can expect ca. 1 m of decrease of the total structural length after the impact. It means that the initial dimension of this supporting truss should be at least 0.5 m larger than the car body (from both sides) in order to protect the upper structure against damage.

The reliability of adaptive structures should be also analysed, especially, with respect to a random failure of actively controlled dissipaters. Setting the stress level triggering plastic-like yielding in adaptive member above the computed value will not cause worse situation in our dissipative adaptation than in passive case. However, setting this level below the computed value can be naturally dangerous.

2. Evolution of the design concept for dynamically adaptive structures

The discussed problem formulation has been developed during the last couple of years. First, it was defined as a quasi-static problem of structural adaptation to extreme loads. A numerically efficient, VDM-based algorithm for optimal design of: (i) location of structural fuses and (ii) yield stress levels in dissipaters, has been proposed in [16], where the following conclusions have been formulated.

(i) The ability of impact energy dissipation for adaptive structure can be significantly increased (over three times in the test example presented).

(ii) In real applications, when limitation of the number of dissipaters has to be taken into account, it is reasonable taking k actuators (where k denotes structural redundancy), responsible for the stress redistribution and another k, responsible for geometrically variable modes of virtual distortions.

(iii) It is preferable to include two dissipaters into each section (every section has one degree of redundancy) of the testing truss cantilever example.

(iv) It is preferable to apply the two step control strategy: (a) accumulating strain energy through stress redistribution using k dissipaters (one dissipater per one section) and then (b) releasing it in a controlled way, using another k dissipaters (one dissipater per one section), that cause large deformations.

(v) It can be observed that the main contribution of the group of adaptive members controlling stress redistribution to the objective function (the global energy dissipation) is given by members from the underloaded sections. On the contrary, the contribution of adaptive elements, causing geometrically variable deformations to the objective function, is mainly due to elements located in the overloaded area. The contribution of the second group of elements is much larger; however, it provokes an undesired increase of the overall structural deformation and has to be controlled. It is important to combine both phases: the strain energy accumulation due to stress redistribution and then the strain energy release due to the plastic-like hinge generation, in order to get a significant energy dissipation.

(vi) If the load is unknown (as in the normal case of active control) then the following strategy in design of adaptive structures can be recommended:
   (a) selection of the best configuration of k active elements, giving the biggest contribution to the objective function for the expected, dominant load distribution;
   (b) selection of k additional active elements, responsible for progressive deformation (e.g., maximally loaded members from each section can be chosen);
   (c) an optimal programming problem has to be solved (Ref. [16], for the determined active element positions and for the measured current load) to determine stress yield levels to be fixed in dissipaters.

The dynamic, VDM-based formulation of the structural adaptation problem (transient analysis) has been applied in the further papers [12–15], where the quasi-static accumulation/release control strategy has been generalised and applied to the adaptive structure equipped with at least $2k$ dissipaters. Definition of the *influence matrix* $\boldsymbol{D}$, can be generalised. The dynamic *influence matrix* $\boldsymbol{D}(t-\tau)$ denotes structural dynamic response (at the time instance t) for locally generated impulse (at the time instance τ) of unit virtual distortions. The accumulation/release strategy of impact energy dissipation (generalised from the static case) can be formulated as follows. Assuming yield stresses $\sigma_i^*(\sigma_i^* \leqslant \sigma^{\mathrm{U}})$ as constant in time, defined for each dissipater separately as control parameters, let us postulate that the scenario of the dissipater's activity can be divided into two stages. In the first one (for $t<T$) maximal accumulation of strain energy is performed taking into account the control parameters ε_i^0 only in the set of overloaded members $(|\sigma_i| \geqslant \sigma_i^*)$. On the other hand, in the second stage, maximal release of strain energy is performed due to action of all dissipaters for $t<T$. The overall behaviour of the structure in the first stage of energy accumulation corresponds to process of elasto-plastic adaptation (except of unloading cases) to yield stresses σ_i^*. Then, taking into account additional search for the best distribution of σ_i^* among active members, the best strategy of dissipater's control can be proposed. The time T corresponds to the instant, when the structure starts to change the movement direction. The following conclusions come from the above generalisation of the quasi-static adaptive structure design concept to the dynamic case:

(i) The contribution of the group of adaptive members controlling stress redistribution to the objective function (the global energy dissipation) decreases for higher impact velocities.

(ii) The structural crash capacity (tested numerically on a model of train car supporting structure, Fig. 1a) reached for the case of stress limits $\sigma_i^* = \sigma^{\mathrm{U}}$ uniformly distributed can be improved through the optimal control strategy of the yield stress levels $\sigma_i^*(\sigma_i^* \leqslant \sigma^{\mathrm{U}})$ in particular elements. For example, for the impact velocity $v = 6\,\mathrm{m/s}$, over 30% increase of the energy dissipation can be reached in this way, due to lowering of the σ_i^* levels in members located in the middle of the car.

(iii) The limit for the structural crash capacity of the same numerical model of railway car supporting structure has been reached at the impact velocity $v = 8\,\mathrm{m/s}$. The yield stress limit σ^{U} has been reached in a passive member during the crash scenario in this case. The optimisation procedure for control of σ_i^* does not help in this case.

A natural continuation of the research undertaken in this paper tends to:

- application of dynamic structural fuses in *all members* and testing the structural crash capacity (constrained by limits on a value of plastic-like distortions ε^{0U} reached in a member);
- development of a methodology for design of adaptive structures with actively controlled properties of dissipaters.

It will be demonstrated, that the application of the above formulation of the dynamic structure adaptation can improve significantly the structural crash capacity. The reason for this improvement comes from the fact that application of only $2k$ dissipaters (as in the quasi-static case) is no longer so effective in the dynamic case. The rank of the static influence matrix determining stress redistribution $[\boldsymbol{D}-\boldsymbol{I}]$ is equal to k (only k linearly independent self-equilibrated stress fields can be induced) and so, additional dissipaters (above the number k) can freely generate kinematic movements causing high-energy dissipation. Contrary, the rank of the dynamic influence matrix determining stress redistribution $[\boldsymbol{D}-\boldsymbol{I}]$ is equal to n (where n is the number of all structural members) as it denotes dynamic structural response calculated with use of the so-called *effective stiffness matrix* (a combination of the original stiffness matrix $\boldsymbol{K}$ and the mass matrix $\boldsymbol{M}$, where rank $(\boldsymbol{M})=n$).

3. VDM-based dynamic analysis of ideal adaptive structures

Let us now formulate the VDM-based description of dynamic analysis of ideal elasto-plastic truss structure. Applying discretised time description the evolution of stresses and deformations can be expressed as follows:

$$\varepsilon_i(t) = \varepsilon_i^{\mathrm{L}}(t) + \varepsilon_i^{\mathrm{R}}(t) = \varepsilon_i^{\mathrm{L}}(t) + \sum_{\tau=\tau_0}^{t} \sum_j D_{ij}(t-\tau)\Delta\varepsilon_j^0(\tau), \tag{1}$$

$$\sigma_i(t) = \sigma_i^{\mathrm{L}}(t) + \sigma_i^{\mathrm{R}}(t) = \sigma_i^{\mathrm{L}}(t) + \sum_{\tau=\tau_0}^{t} \sum_j E_i[D_{ij}(t-\tau) - \delta_{ij}]\Delta\varepsilon_j^0(\tau), \tag{2}$$

where the so-called *dynamic influence matrix* $D_{ij}(t-\tau)$ describes the strain evolution caused in the truss member i and in the time instance $\tau \geqslant 0$, due to the unit *virtual distortion* impulse $\Delta\varepsilon_j^0(\tau) = 1$ generated in the member j in the time instant $\tau \cdot \Delta\varepsilon_i^0(t) = \dot{\varepsilon}_i^0(t)\Delta t$ and i runs through all members of truss structure. The vector $\sigma_i^{\mathrm{L}}(t)$ denotes the stress evolution due to the external load applied to elastic structure. Note that the matrix $\mathbf{D}$ stores information about the entire structure properties (including boundary conditions) and describes dynamic (not static) structural response for locally generated impulse of virtual distortion.

The equation of motion of a truss structure with virtual distortions generated in members can be expressed in the following form (cf. [15]):

$$M_{ij}\ddot{u}_j + C_{ij}\dot{u}_j + \sum_k H_{ik}A_k l_k E_k(\varepsilon_k - \varepsilon_k^0) = P_i, \tag{3}$$

where $\boldsymbol{M}_{ij}$, $\boldsymbol{C}_{ij}$ and $\boldsymbol{H}_{ij}$ denote the mass, natural damping and structural connectivity matrices, respectively, A_i and l_i denote element cross-sections and length, respectively. Excitation is time dependent. To simplify the further calculations it was assumed that natural damping is equal to zero, $C_{ij} \equiv 0$.

The dynamic analysis of elasto-plastic structure with the following yield conditions:

$$|\sigma_i(t)| \leqslant \sigma^{\mathrm{U}} \tag{4}$$

can be performed through an integration approach (e.g., the Newmark's method) with the plastic adaptation effect simulated through virtual distortions at every time step when constraints (4) are violated. This modelling of plastic adaptation requires solving of the following set of linear equations:

$$\sigma_i(t) = \sigma_i^{\mathrm{L}}(t) + \sum_{\tau=\tau_0}^{t} \sum_j E_i[D_{ij}(t-\tau) - \delta_{ij}]\Delta\varepsilon_j^0(\tau) = \sigma^{\mathrm{U}} \tag{5}$$

for indices i and j running through the set of all, already plastified and still over-loaded members determining corresponding increments of virtual, plastic-like distortions $\Delta\varepsilon_j^0$. The analogous increments for time instances t should be determined in previous time steps $(t<\tau)$ of the dynamic analysis. The numerical advantage of the proposed approach comes from the fact, that having stored pre-computed influence matrices, elasto-plastic dynamic analysis requires only solving linear Eq. (5) instead of iterative searching for response satisfying violated constraints (4). This cost of plastic adaptation is particularly cheap if number of overloaded members is small. The flow chart of the VDM-based dynamic elasto-plastic analysis is shown in Table 1.

Alternatively, the simulation of plastic adaptation through virtual distortions can be performed on the base of variational approach postulating minimisation of energy dissipation in overloaded elements at every time step when constraints (4) are violated. The problem

$$\min \mathrm{U} = \min \sum_{t=0}^{T} \sum_i A_i l_i \sigma_i(t) \Delta\varepsilon_i^0(t) \tag{6}$$

s.t.

$$|\sigma_i(t)| \leqslant \sigma^{\mathrm{U}}, \quad \sigma_i(t)\Delta\varepsilon_i^0(t) \geqslant 0, \tag{7}$$

where $\sigma_i(t)$ is determined by Eq. (2)and i runs through already plastified members, leads to the same results as the simulation problem (5), what follows also from general theorems of plasticity (c.f. Ref. [11]).

Note, that the non-linear programming problem (6) and (7) with respect to the control parameters $\Delta\varepsilon_i^0(\tau)$ can be solved through a gradient method with derivatives analytically determined. The derivative for the objective function (6) is

$$\frac{\mathrm{d}U}{\mathrm{d}\Delta\varepsilon_j^0(\tau)} = A_j l_j \sigma_j(\tau) + \sum_i A_i l_i \frac{\mathrm{d}\sigma_i(t)}{\mathrm{d}\Delta\varepsilon_j^0(\tau)} \Delta\varepsilon_i^0(t), \tag{8}$$

where

$$\frac{\mathrm{d}\sigma_i(t)}{\mathrm{d}\Delta\varepsilon_j^0(\tau)} = E_i[D_{ij}(t-\tau) - \delta_{ij}],$$

Table 1
Flow-chart of the VDM-based dynamic elasto-plastic analysis (VDM/D)

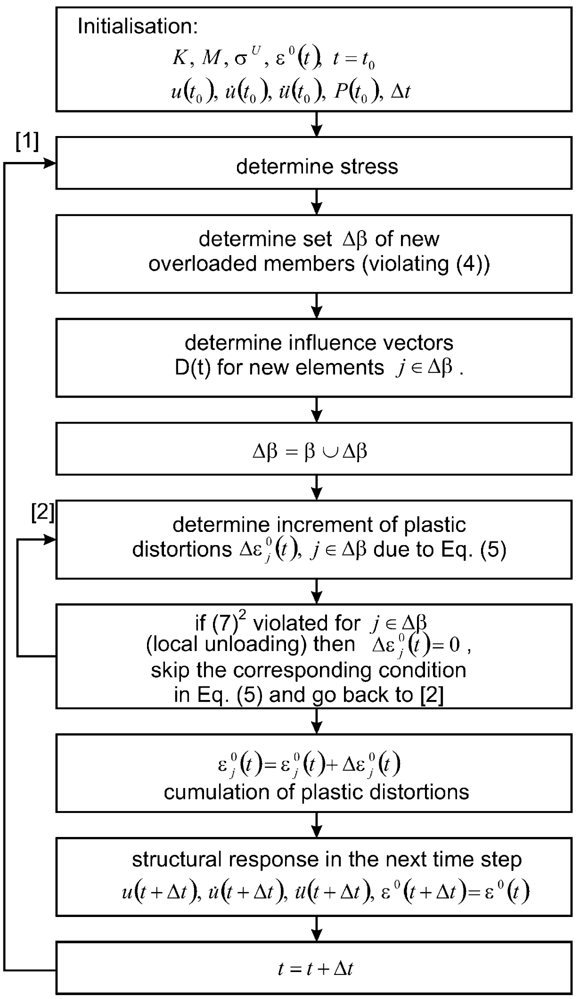

while derivative for side constraint $(7)^2$ takes the form

$$\frac{\mathrm{d}\sigma_i(t)\Delta\varepsilon_i^0(t)}{\mathrm{d}\Delta\varepsilon_j^0(\tau)} = \sigma_i(t)\delta_{ij}\delta(t-\tau) + E_i[D_{ij}(t-\tau) - \delta_{ij}]\Delta\varepsilon_i^0(t), \tag{9}$$

where $\delta(t-\tau)$ is equal to 1 for $t = \tau$ and 0 for other arguments.

Numerical verification of results obtained with the VDM-based code (variational problem (6) and (7) solved through the Powell procedure [19]) vs. standard codes (MARC and ABAQUS) performed on the crash example described below (cf. Fig. 9) is presented below.

In the case of small deformations, the VDM/D (VDM Dynamics) code simulates development of plastic zone without necessity of plastic response iteration in every time step and stiffness matrix reformation. The numerical efficiency of this approach is still higher in the case of gradient-based methodology used in structural remodelling when analytically based sensitivity analysis is taken into account (cf. Eqs. (8) and (9)).

The following measure has been used to compare values of structural responses simulated by two commercial programs ABAQUS, MARC and the VDM/D:

$$\mathrm{MR} = \left| \frac{V_{\mathrm{ABAQUS}} - V_{\mathrm{MV}}}{V^{\mathrm{MAX}}_{\mathrm{ABAQUS}}} \right| 100\%,$$

where V_{ABAQUS} and V_{MV} corresponds to the results obtained with the ABAQUS programme and MARC or VDM/D, respectively. $V^{\mathrm{MAX}}_{\mathrm{ABAQUS}}$ is maximum value of the quantity simulated with ABAQUS. The proposed measure MR of results dispersion allows to compare results related to maximally overloaded elements (therefore critical for the overall structural safety).

The truss structure shown in Fig. 9 represents a simplified model of supporting frame of railway vehicle. It is assumed uniform distribution of cross-sectional areas $A_i = 0.00244\,\mathrm{m}^2$

Table 2
Testing results: (a) stresses and (b) plastic distortions

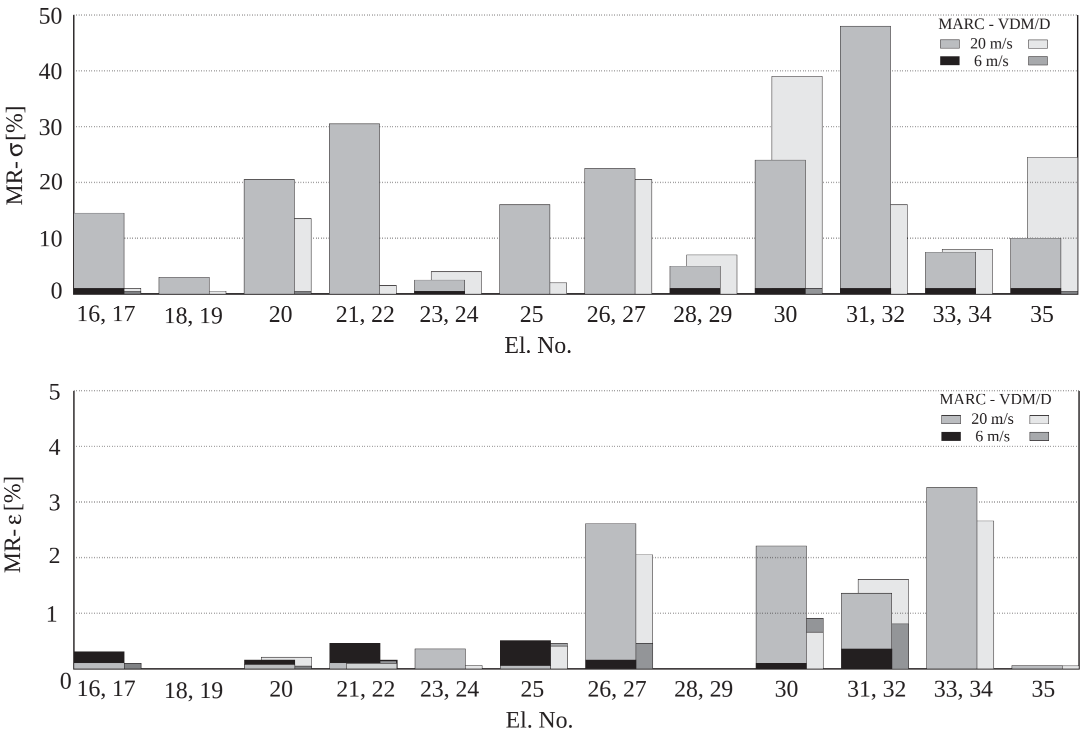

Impact velocities 6 and 20 m/s.

(for $i = 1 \ldots 35$), plastic yield stress $\sigma^U = 200$ MPa, the Young's modulus $E_i = 2.1 \times 10^5$ MPa and the material density $\rho_i = 7800$ kg/m^3. Two cases have been analysed. The first one is when the structure hits the rigid wall with the initial velocity 6 m/s. The small deformations model leads to very similar results obtained by all three numerical tools (Table 2). Numbers of structural elements shown in Fig. 8 are marked on the horizontal lines of Table. In the case of impact with an initial velocity of 20 m/s, a large deformations model has been used and the numerical results obtained for VDM/D, MARC and ABAQUS are presented in Table 2 and Figs. 2–7. Note that results obtained with VDM/D are in between those obtained with ABAQUS and MARC.

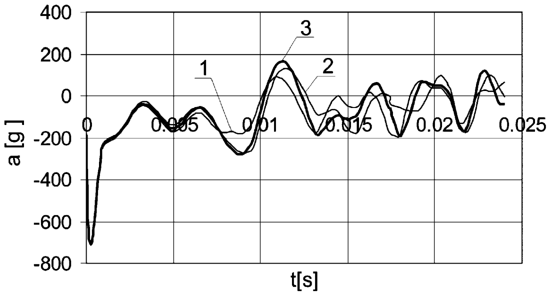

Fig. 2. Horizontal accelerations for joint 14 (1-Abaqus, 2-Marc, 3-VDM/D).

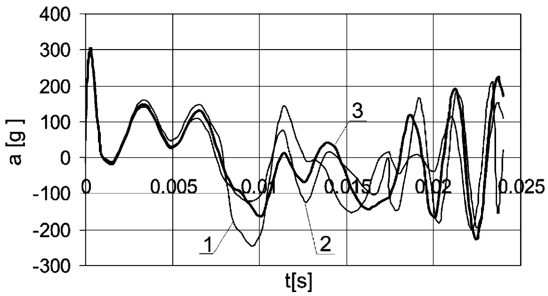

Fig. 3. Vertical accelerations for joint 14 (1-Abaqus, 2-Marc, 3-VDM/D).

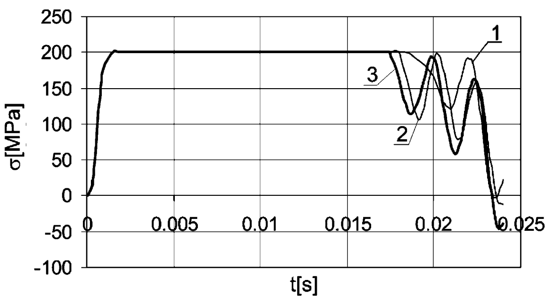

Fig. 4. Fluctuations of stresses in element 30.

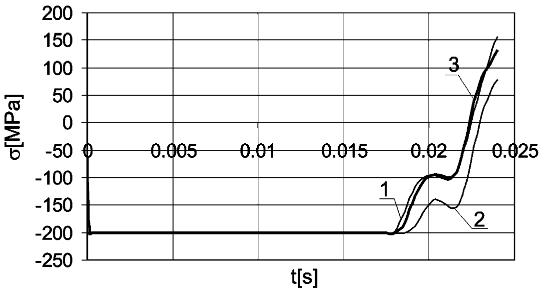

Fig. 5. Fluctuations of stresses in element 31.

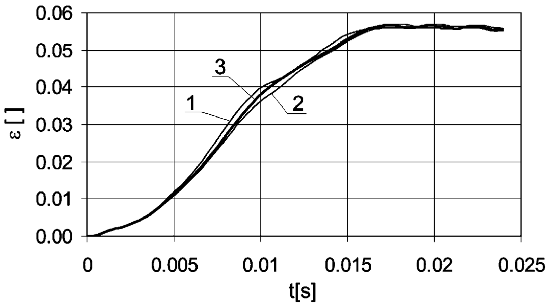

Fig. 6. Development of plastic distortions in element 30.

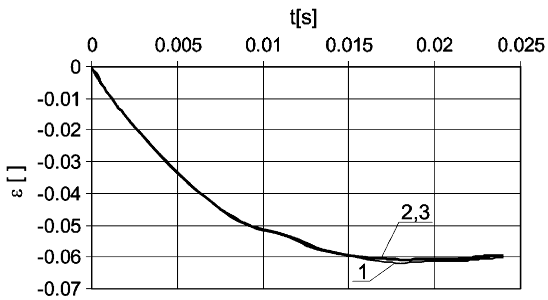

Fig. 7. Development of plastic distortions in element 30.

Dispersion of results for higher impact velocities and higher time steps can be observed. However, to choose the most realistic simulation, verifications vs. some experiment should be taken into account.

4. Crashworthiness of adaptive structure with constant properties of dissipaters

The concept of adaptive crashworthiness will be now tested demonstrating load capacity of the following adaptive structures, equipped with controlled energy dissipaters:

(a) structures with fixed material distribution and stress limits $\sigma^* = \sigma^{\mathrm{U}}$ triggering plastic-like behaviour of dissipaters;

(b) structures with fixed stress limits $\sigma^* = \sigma^{\mathrm{U}}$ and material distribution remodelled to maximise load capacity;
(c) structures with fixed material distribution and stress limits σ^* tuned to maximise load capacity.

To determine maximal crash safe velocity of adaptive structure (equipped with elasto-plastic-like structural fuses in all elements) let us consider again the truss model of railway car supporting frame with the total mass 1450 kg (Fig. 8) hitting the rigid wall. Assuming that the members' cross-sections ($A_i = 0.00244\ \mathrm{m}^2$ for all $i = 1, \ldots, 35$), the yield stresses (constant in time and equal for all elements), $\bar{\sigma}_i^{\mathrm{U}} = 200\ \mathrm{MPa}$ are determined, the Young modulus $E_i = 2.1 \times 10^5\ \mathrm{MPa}$ and the material density $\rho_i = 7800\ \mathrm{kg/m^3}$, the crash scenario for a given train velocity can be performed through the VDM-based dynamic elasto-plastic analysis (VDM/D). To determine the maximal safe velocity the algorithm shown in Table 3 has been applied, where

$$\varepsilon_i^0(t) \leqslant \bar{\varepsilon}^0 \tag{10}$$

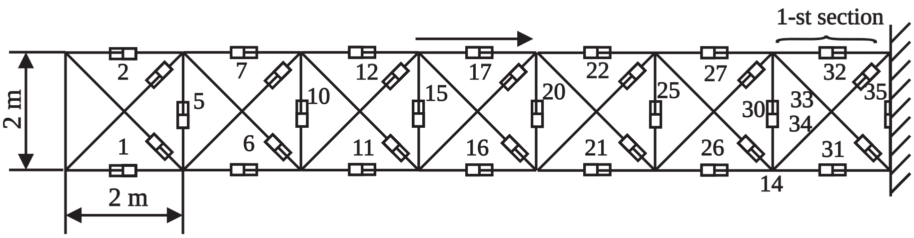

Fig. 8. Adaptive structure.

Table 3
Flow-chart of the algorithm determining maximal safe impact velocity for adaptive structure ($\sigma_i^* = \sigma^{\mathrm{U}} = \mathrm{const}$; $A_i = \mathrm{const}$ case)

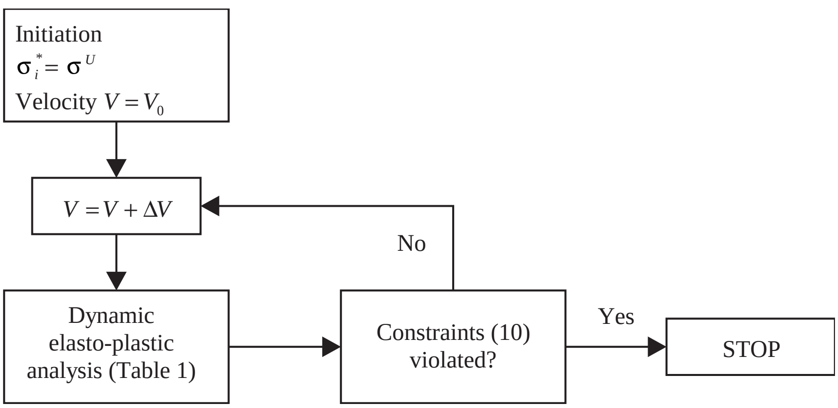

and $\bar{\varepsilon}_i^0 = 0.1$ denotes limits imposed on plastic-like distortions generated in structural members. The applied time step is $t = 0.0003$ s. The maximal impact velocity $V_{\mathrm{MAX}} = 25.2$ m/s has been realised and the resulting plastic distortions are shown in Table 4.

Almost 98% of the initial kinetic energy 460 kJ has been dissipated after $t = 0.024$ s. The energy dissipation effect is demonstrated in Fig. 9. Figs. 10 and 11 show fluctuations of stresses during the whole dissipation process in active members of the structure (with the constant stress limit $\bar{\sigma}_i^{\mathrm{U}} = 200$ MPa). The evolution of the corresponding plastic-like virtual distortions is presented in Figs. 12 and 13. Additionally, the strain recoverable energy distribution through the structural sections is shown in Fig. 14.

Table 4
Values of stress limits and plastic distortions in elements of the structure

El. No.	21, 22	23, 24	25	26, 27	28, 29	30	31, 32	33, 34	35
Stress limits σ_i^{U} (MPa)	200	200	200	200	200	200	200	200	200
Plastic distortions ε_i^0	−0.0201		0.0015	−0.0043		0.0837	−0.0997	−0.0282	0.0007

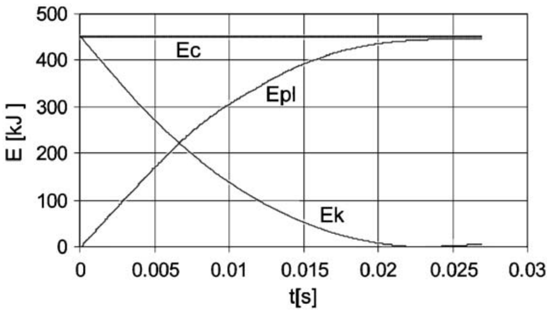

Fig. 9. Redistribution of the energy components during the crush.

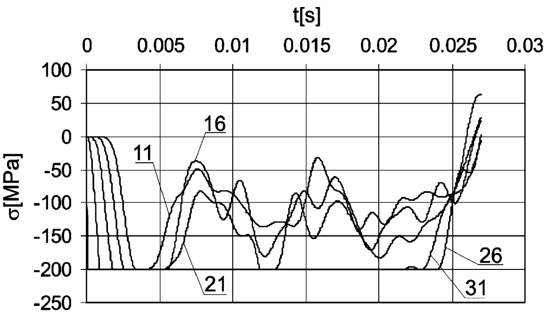

Fig. 10. Fluctuation of stresses in compressed, horizontal, active members of the adaptive structure.

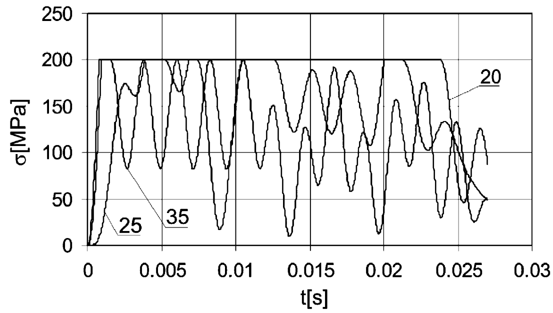

Fig. 11. Fluctuation of stresses in tensioned, vertical, active members of the adaptive structure.

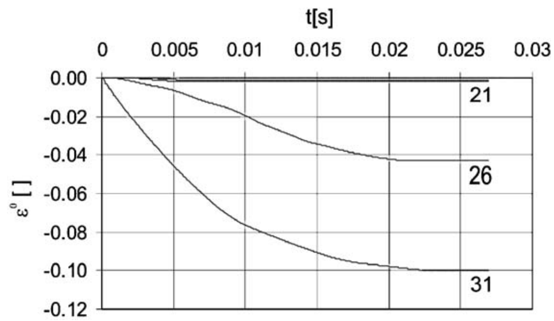

Fig. 12. Evolution of plastic-like virtual distortions in active horizontal members.

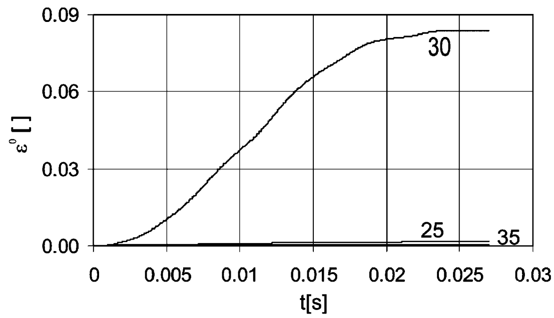

Fig. 13. Evolution of plastic-like virtual distortions in active vertical members.

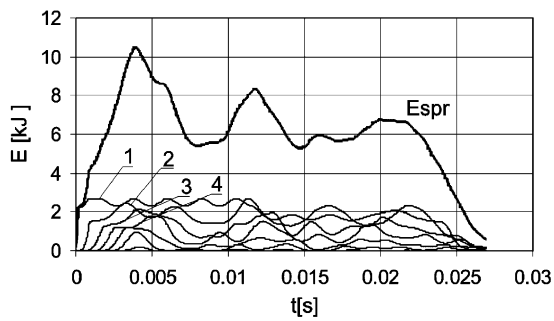

Fig. 14. Strain, recoverable energy distribution through sections (e.g., section no. 1 contains members 31–35).

5. Optimal remodelling for the best crashworthiness

Let us now check, how sensitive the above solution is for structural remodelling. To this end, we assume that material distribution (cross-sectional areas A_i) can be modified within the following constraints:

$$\alpha_1 A^0 \leqslant A \leqslant \alpha_2 A^0, \tag{11}$$

where $\alpha_1 = 16.67\%$ and $\alpha_2 = 600\%$ has been assumed and the total material volume is constant:

$$\sum_i A_i l_i = \sum_i A^0 l_i = \text{const.} \tag{12}$$

The algorithm allowing redesign of material distribution to reach the highest safe impact velocity is shown in Table 5.

To improve design variables in over-distorted elements the following formulas can be applied (until constraints (11) are satisfied):

$$A_i = A_i + g_i \Delta, \tag{13}$$

where the penalty function:

$$g_i = \frac{|\varepsilon_i^{0\ \mathrm{MAX}} - \varepsilon^{\mathrm{U}}|}{\varepsilon^{\mathrm{U}}}. \tag{14}$$

$\varepsilon_i^{0\ \mathrm{MAX}}$ is the maximal value of ε_i^0 taken in the dynamic process and Δ denotes the applied design step. The above remodelling results in tracing constraints ε^{U} in over-distorted members. Increasing material volume in over-distorted elements, simultaneously we have to reduce design variables in under-distorted members (proportionally to the weighting coefficients $(\varepsilon^{\mathrm{U}} - (\varepsilon_i - \varepsilon^*)/\varepsilon^{\mathrm{U}})$ satisfying requirement (12).

The above approach (based on the fact that $(\mathrm{d}g_i/\mathrm{d}A_i) \leqslant 0$) can be applied in the first stage of remodelling process. However, when over and under-distorted elements reach their upper and

Table 5
Flow-chart of the algorithm for adaptive structure redesign ($\sigma_i^* = \sigma^{\mathrm{U}} = \text{const}$ case)

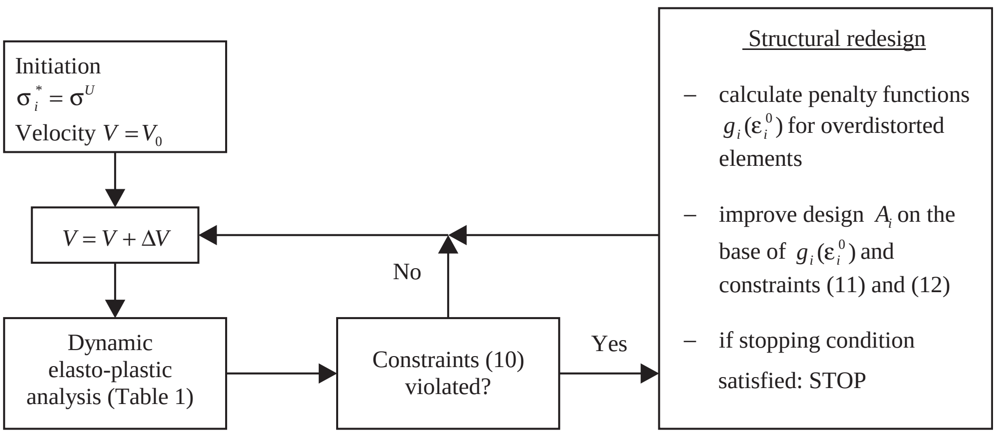

Table 6
Plastic distortions and material distribution reached in remodelled adaptive structure (for maximal safe impact velocity $V_{MAX} = 61.5$ m/s)

El. No.	**1,2**	**3,4**	**5**	**6,7**	**8,9**	**10**	**11,12**	**13,14**	**15**	**16,17**	**18,19**
σ_i^U **[MPa]**	200	200	200	200	200	200	200	200	200	200	200
A_i **[%** A^0**]**	16.7	19,6	19,6	19.7	19.8	19.8	17.1	19.6	23.8	21.6	29.1
ε_i^0				-0.00018		0.00002	-0.04968	-0.00024	0.09786	-0.0989	-0.00013
El. No.	**20**	**21,22**	**23,24**	**25**	**26,27**	**28,29**	**30**	**31,32**	**33,34**	**35**	
σ_i^U **[MPa]**	200	200	200	200	200	200	200	200	200	200	
A_i **[%** A^0**]**	32.1	47.2	58.4	59.6	91.4	96.4	28.2	600	551.8	22.61	
ε_i^0	0.09935	-0.0989		0.09861	-0.1	-0.00142	0.09502	-0.09916	-0.01578	0.0405	

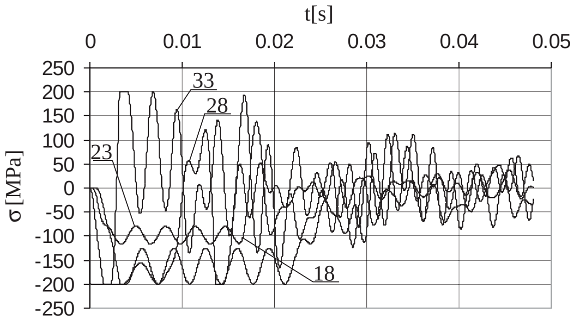

Fig. 15. Fluctuation of stresses in compressed, horizontal, active members of the adaptive structure.

lower design constraints (11) then more precise remodelling tools should be applied. One possibility is to use general gradient calculations dg_i/dA_i in the redesign process.

Testing calculations have been performed, assuming that reaching of limits $\alpha_2 A^0$ and $\alpha_1 A^0$ in first over-distorted and under-distorted elements, respectively, stops redesign procedure. The results are demonstrated in Table 6. Limits reached due to active constraints are marked in bold. The corresponding maximal safe impact velocity is $V_{MAX} = 61.5$ m/s.

Figs. 15–17 show fluctuations of stresses in horizontal, vertical and bracing elements respectively (with the constant yield stress $\sigma^U = 200$ MPa). The evaluation of the corresponding plastic-like distortions (in horizontal, vertical and bracing elements) is presented in Figs. 18 and 19. Additionally, the strain recoverable energy distribution through the structural sections has been shown in Fig. 20.

The material distribution in remodelled structure is shown in Fig. 21. If additionally, the assumption about symmetry of the solution is taken into account, the material distribution shown in Fig. 22 and a maximal safe impact velocity $V_{MAX} = 47$ m/s can be reached.

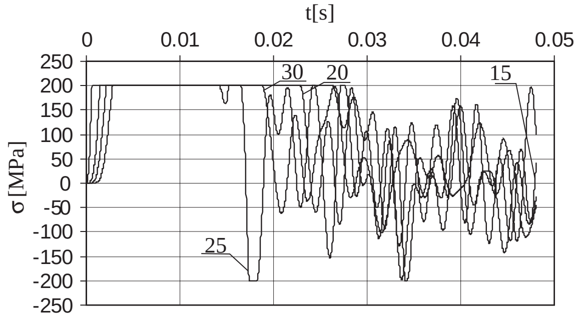

Fig. 16. Fluctuation of stresses in bracing, active members of the adaptive structure.

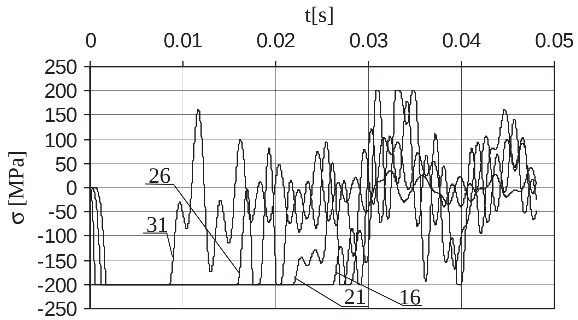

Fig. 17. Fluctuation of stresses in tensioned, vertical, active members of the adaptive structure.

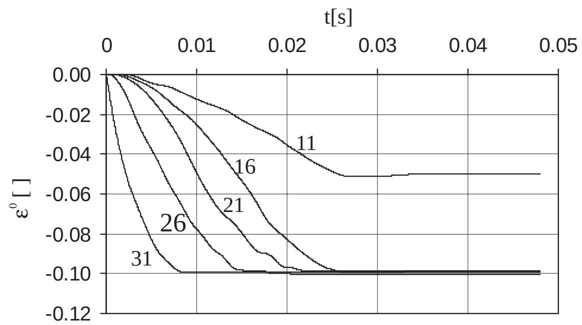

Fig. 18. Evolution of plastic-like virtual distortions in active horizontal members.

The remodelling process based on tracing of active constraints (13) and (14) was stopped when limit values $\alpha_1 A^0$ and $\alpha_2 A^0$ has been reached in elements No. 1, 2 and No. 31, 32, respectively. Table 6 demonstrates that almost the whole structure has been involved in the energy dissipation process. Horizontal as well as vertical elements of the first four sections are distorted up to the limit value $\varepsilon^0 = \varepsilon^{\mathrm{U}}$ (Table 6).

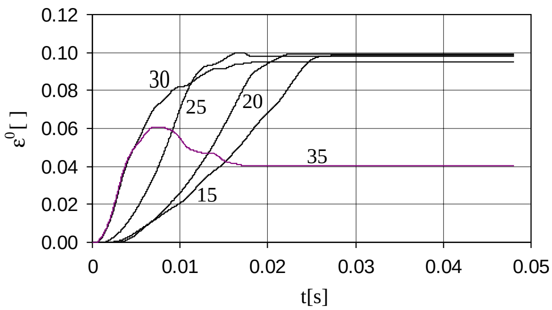

Fig. 19. Evolution of plastic-like virtual distortions in active vertical members.

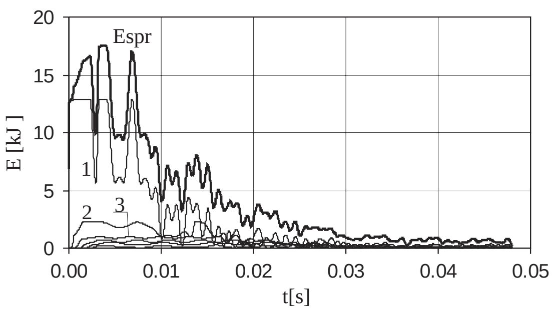

Fig. 20. Strain recoverable energy distribution through structure sections.

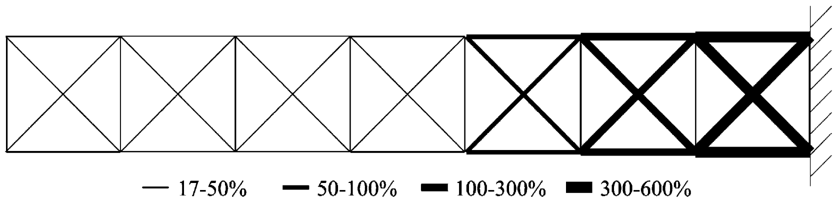

Fig. 21. Material distribution for adaptive structure with maximal crashworthiness (symmetric distribution of material).

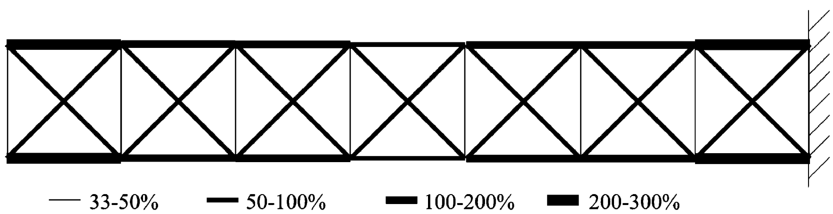

Fig. 22. Material distribution for adaptive structure with maximal crashworthiness.

6. Optimal control of stress limits for the best crashworthiness

The problem of optimal adjustment of the yield stress limits in particular elements of adaptive structure (with fixed material distribution) will be discussed in this section. Assuming the same initial data as in the previously discussed example let us determine stress levels σ_i^* satisfying constraints:

$$\sigma_i^* \leqslant \sigma^{\mathrm{U}} \tag{15}$$

and triggering plastic-like behaviour of dissipaters in such a way that the safe impact velocity is maximised.

To perform the procedure of adaptation of the yield stresses σ_i^* to overloading (at each loading level determined by the impact velocity V, Table 7), solving of the following problem of maximisation of the total energy dissipation is proposed:

$$\max \mathrm{U} = \max \sum_{t=0}^{T} \sum_{i} A_i l_i \sigma_i(t) \Delta\varepsilon_i^0(t) \tag{16}$$

where i runs through already plastified elements, $\sigma_i(t) = \sigma_i(\varepsilon_j^0(t))$ is determined by Eq. (2), and

$$|\sigma_i(t)| \leqslant \sigma_i^* \leqslant \sigma^{\mathrm{u}}, \quad \sigma_i(t)\Delta\varepsilon_i^0(t) \geqslant 0, \quad \left|\varepsilon_i^0(t)\right| \leqslant \varepsilon^{\mathrm{u}}. \tag{17}$$

Starting the adaptation procedure from the upper bound of design variables $\sigma_i^* = \sigma^{\mathrm{U}}$ and making use of gradients $\mathrm{dU}/\mathrm{d}\sigma_i^*$ the gradual modification (mostly reduction) of local yield stress levels σ_i^* can be performed due to the formula:

$$\sigma_i^{*\mathrm{NEW}} = \sigma_i^* + \frac{\mathrm{dU}}{\mathrm{d}\sigma_i^*}\Delta \tag{18}$$

Table 7
Flow-chart of the algorithm for yield stress levels redesign ($\mathrm{A}_i = \mathrm{A}^0 = \mathrm{const}$ case)

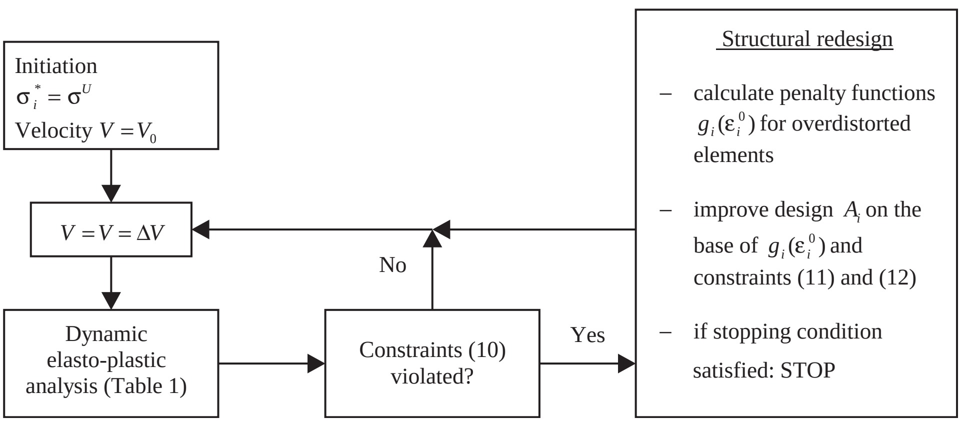

(where Δ is arbitrarily chosen through numerical experiment) for all elements with no active constraints $(17)^1$ and $(17)^2$. We assume that a stationary condition is reached if:

- constraint $(17)^1$ is active for at least one member;
- constraint $(17)^3$ is active for at least one "fully distorted" member of each of 7 structural sections;
- $(\mathrm{d}U/\mathrm{d}\sigma_i^*) = 0$ or further modification of design variables σ_i^* for each element causes violation of constraint $(17)^3$ in "fully distorted" element in the section.

For a certain load level, generated by the impact velocity V^1, the solution of optimisation problem (16) and (17) does not exist. It means that the previously found structural adaptation corresponds to the maximal safe impact velocity V^{MAX}.

The numerical results obtained for the above-discussed supporting frame of railway vehicle are presented below. The optimal distribution of yield stress levels σ_i^* and the corresponding cumulated plastic distortions determined for the maximal safe impact velocity $V^{\mathrm{MAX}} = 32\ \mathrm{m/s}$ are presented in Table 8. The energy dissipation effect is demonstrated in Fig. 23 while the distribution of recoverable component of strain energy in the sequence of truss sections is shown in Fig. 24. Figs. 25 and 26 show fluctuations of stresses in active horizontal and vertical elements, respectively. The evolution of the corresponding plastic-like distortions (in horizontal and bracing

Table 8
Stress yield levels and cumulated plastic distortions reached in optimally adopted structure for maximal safe impact velocity $V^{\mathrm{MAX}} = 32\ \mathrm{m/s}$

El. No.	**1,2**	**3,4**	**5**	**6,7**	**8,9**	**10**	**11,12**	**13,14**	**15**	**16,17**	**18,19**
σ_i^U **[MPa]**	9,35	9,05	9,36	6,25	9,06	19,4	20,6	16,7	26,1	49,1	18,9
ε_i^0			0,00001	-0,0997	-0,0497	0,0003	-0,0998	-0,0496	0,0007	-0,0993	-0,0459
El. No.	**20**		**23,24**	**25**	**26,27**	**28,29**	**30**	**31,32**	**33,34**	**35**	
σ_i^U **[MPa]**	41,2	73,5	41,0	68,1	126	48,1	114,1	190	108,6	200	
ε_i^0	0,014	-0,0978	-0,045	0,0011	-0,0986	-0,0472	0,0072	-0,0979	-0,0471		

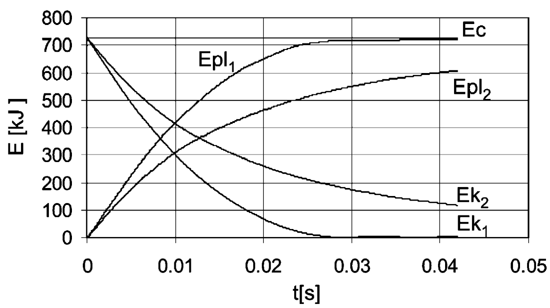

Fig. 23. Redistribution of the energy components (k—kinetic, pl—plastic deformation) during the crush for case 32 m/s (1—unmodified, 2—modified stresses limits).

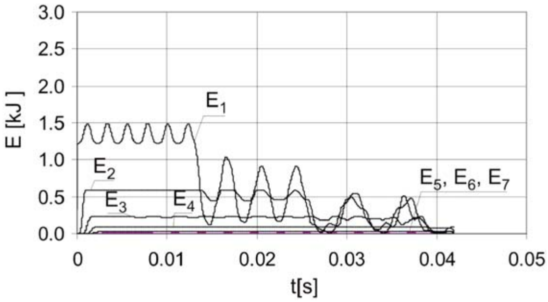

Fig. 24. Strain, recoverable energy distribution through sections (e.g., section no. 1 contains members 31–35).

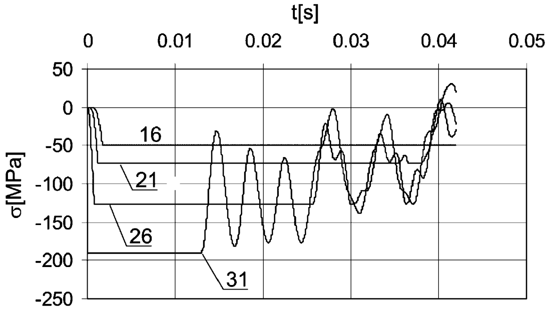

Fig. 25. Fluctuation of stresses in compressed, horizontal, active members of the adaptive structure.

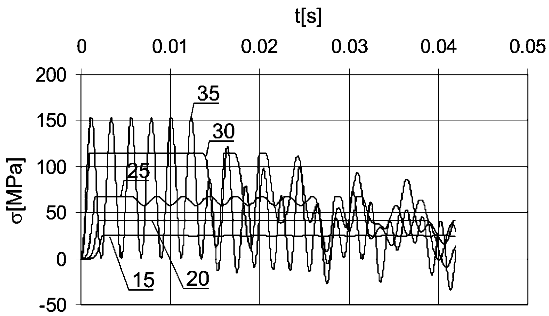

Fig. 26. Fluctuation of stresses in tensioned, vertical, active members of the adaptive structure.

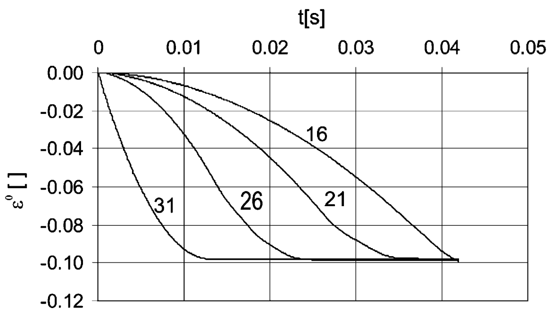

Fig. 27. Evolution of plastic-like virtual distortions in active horizontal members.

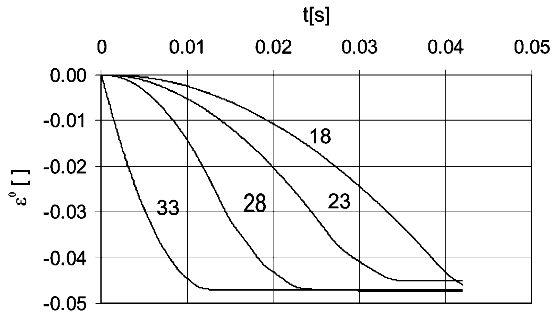

Fig. 28. Evolution of plastic-like virtual distortions in active bracing members.

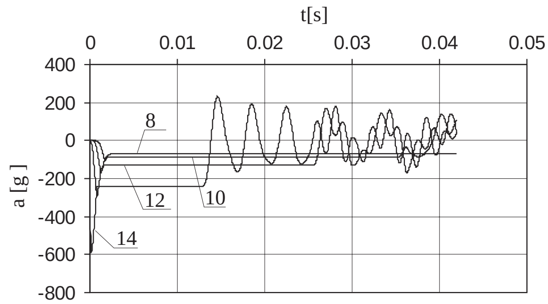

Fig. 29. Evolution of horizontal accelerations in node nos. 8, 10, 12 and 14 of structure (modified stress yield limits—32 m/s).

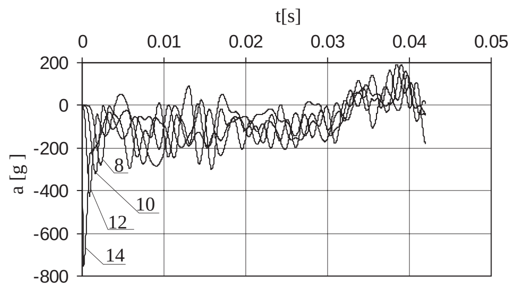

Fig. 30. Evolution of horizontal accelerations in node nos. 8, 10, 12 and 14 of structure (unmodified stress yield limits—25.2 m/s).

elements) is shown in Figs. 27 and 28, respectively. Accelerations of structural nodes for two considered cases (32 and 25.2 m/s) are shown in Figs. 29 and 30, respectively.

7. Conclusions

On the basis of the numerical examples presented above, the following generalised, quantitative conclusions can be formulated [20]:

- properly designed adaptive structure (equipped with controllable dissipaters—“structural fuses”) can behave similarly to ideal elasto-plastic structures.

- the overall crashworthiness of such adaptive structures can be significantly improved with respect to "passive" structures.
- adjustment of controlled members stress limits triggering plastic-like distortions to predicted impact can still improve significantly the overall structure crashworthiness.
- remodelling of adaptive structure (modification of material distribution) can give higher energy dissipation effect. However, this is applicable to only one impact scenario.

We can expect that qualitative results obtained for a truss structure can be generalised for any of frame structure or structures composed of continuous elements. Note that the controllable scenario of adaptation to crush leads to qualitatively different structural deformation schemes (Fig. 31) for different structural design.

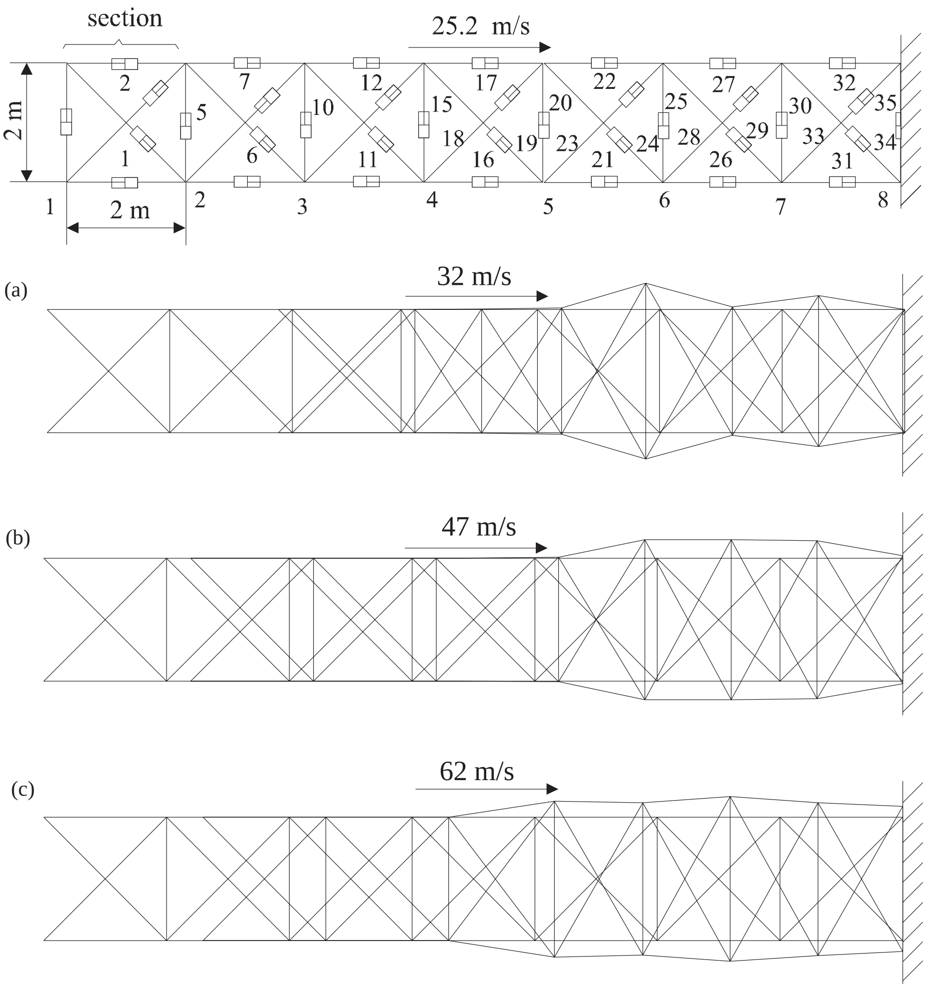

Fig. 31. Impact scenario (a) 32 m/s, (b) 47 m/s (symmetrical mass distribution) and (c) 61 m/s (general mass distribution case).

It follows from the above discussion a list of requirements:

- Further development of the VDM/D approach will improve its ability to perform optimisation of adaptive structures for best crashworthiness.
- There is need for experimental verification of numerical tools for non-linear fast-dynamics structural analysis.
- In order to utilise proposed improvements in practice, there is a need for technical solutions capable of realising controllable dissipation effect in structural elements or joints (e.g., proportional valves in hydraulic pistons).
- In a general methodology of design of adaptive structures for best crashworthiness, it is reasonable:

(a) Firstly, to design material distribution (remodelling process) in adaptive structure for most probable impact loading.
(b) Secondly, to apply (in real time) the optimally designed (due to predicted impact) yield stress levels in controlled dissipaters.

Finally, note that the proposed adaptive crashworthiness concept can be applied not only to protect vehicles against collisions, but also in design of high impact absorbing microstructures (e.g., materials protecting against explosions).

Acknowledgements

This work was supported by the grant no. 5T07A05222 from the Institute of Fundamental Technological Research, Poland, funded by the National Research Committee and presents a part of the Ph.D. thesis of the second author, supervised by the first author [18].

References

[1] Lewis J. Tests validate methods to cut injuries. Int Railway J Res Dev 1995; 30–1.
[2] SNCF Report: Succes complet de collision experimentale sur TGV 2N, Revue generale des chemins de fer, April 1994. p. 41–3.
[3] Cleon LM. Crashworthiness of new design railways vehicles. Proceedings of the International Symposium on Technological Innovation in Guided Transports, Lille, France, 1993.
[4] Abramowicz W, Jones N. Transition from uniform bending to progressive buckling of tubes loaded statically and dynamically. Int J Impact Eng 1997;19(5–6):415–37 [Special issue in honour of Professor W. Johnson's 75th birthday].
[5] Abramowicz W, Wierzbicki T. Calculation and design of multi-cell aluminium structures for crash. Final Report to the JRC/BRITE EuRam II project on "Low Weight Vehicle—Design of Aluminium Alloy Body Structures", February 1994.
[6] Distin K, Smith RA. Rail vehicle crashworthiness and the role of FE analysis. PAM'93 Third European Workshop on Advanced Finite Element Simulation Techniques, Schlagenbad, Germany, 1993.
[7] Locomotive Crashworthiness Research, US Department of Transportation, Federal Railroad Administration. Final Report DOT/FRA/ORD-95/08.1, DOT-VNTCS-FRA-95-4.1, vols. 1–5, 1995.
[8] Tyrell DC, Severson KJ, Marquis BP. Train crashworthiness for occupant survivability, crashworthiness and occupant protection in transportation systems. Am Soc Mech Eng 1995; AMD-Vol. 210/BED-Vol. 30: 59–78.

[9] Smith RA. Crashworthiness of trains: principles and progress, crashworthiness and occupant protection in transportation systems. Am Soc Mech Eng 1995; AMD-Vol. 210/BED-Vol. 30: 79–88.
[10] Abramowicz W. The macro element approach in crash calculations. In: Ambrosio J, Pereira M, editors. Crashworthiness of transportation systems: structural impact and occupant protection. Kluwer: Dordrecht; 1997.
[11] Holnicki-Szulc J, Gierlinski JT. Structural analysis, design and control by the VDM method. Chichester: Wiley; 1995.
[12] Knap L, Holnicki-Szulc J. Dynamic analysis of adaptive, visco-plastic structures. Proc Complas Barcelona 1997;5:17–9.
[13] Holnicki-Szulc J, Knap L, Flont P. Adaptive structures-general concept and railway applications. Proceedings of the Second International Conference MV2 on Active Control in Mechanical Engineering, Lyon October 1997. p. 22–3.
[14] Knap L, Holnicki-Szulc J. Smart structures with adaptive impact absorption. Proceedings of the Second World Congress of Structural and Multidisciplinary Optimization, Zakopane, Red Gutkowski, Mróz May 1997. p. 26–30.
[15] Knap L, Holnicki-Szulc J. Design of adaptive structures for improved crashwortheness. Proceedings of the NATO Advanced Research Workshop SMART-98, Pultusk, Czerwiec, 1998. p. 16–19.
[16] Holnicki-Szulc J, Mackiewicz A, Kolakowski P. Design of adaptive structures for improved load capacity. AIAA J 1998;36(3):471–6.
[17] Spencer Jr BF, David Carlson J, Sain MK, Yang G. On the current status of magnetorheological dampers: seismic protection full-scale struct. Proceedings of the American Control Conference, Albuquerque New Mexico, June 1997. p. 4–6.
[18] Adaptive Impact Absorption, IFTR, Patent licence applied for.
[19] Powell MJD. Tolmin: a Fortran package for linearly constrained optimization calculations, report DAMTP/1989/NA2. Cambridge, UK: University of Cambridge; 1989.
[20] Knap L, Holnicki-Szulc J. Optimal design of adaptive structures for the best crashworthiness. Proceedings of the Third World Congress on Structural and Multidisciplinary Optimization, Buffalo, May 1999.